Kaplan, M. R., & Simoni, R. D. (1985) *J. Cell Biol. 101*, 441-445.
Kasper, A. M., & Helmkamp, G. M., Jr. (1981) *Biochim. Biophys. Acta 664*, 22-32.
Kates, M. (1972) in *Techniques in Lipidology*, pp 393-394, North-Holland, Amsterdam.
Kremer, J. M. H., Van der Esker, M. W. J., Pathmamanoharan, C., & Wiersma, P. H. (1977) *Biochemistry 16*, 3932-3934.
Levade, T., Salvayre, R., & Gatt, S. (1987) *Experienta 43*, 1002-1006.
Massey, J. B., Gotto, A. M., & Pownall, H. J. (1982) *Biochemistry 21*, 3630-3636.
Massey, J. B., Hickson, D., She, H. S., Sparrow, J. T., Via, D. P., Gotto, A. M., & Pownall, H. J. (1984) *Biochim. Biophys. Acta 794*, 274-280.
Massey, J. B., Hickson, D., She, H. S., Sparrow, J. T., Via, D. P., Gotto, A. M., & Pownall, H. J. (1985) *Biochim. Biophys. Acta 835*, 124-131.
Michell, R. H. (1975) *Biochim. Biophys. Acta 415*, 81-147.
Nichols, J. W., & Pagano, R. E. (1982) *J. Biol. Chem. 258*, 5368-5371.
Patel, K. M., Morrisett, J. D., & Sparrow, J. T. (1979) *J. Lipid Res. 20*, 674-677.
Patton, J. M., Fasulo, J. M., & Robins, S. J. (1982) *J. Lipid Res. 23*, 190-196.
Roseman, M. A., & Thompson, T. E. (1980) *Biochemistry 19*, 439-444.
Rouser, G., Fleischer, S., & Yamamoto, A. (1970) *Lipids 5*, 494-496.
Singleton, W. S., Gray, M. S., Brown, M. L., & White, J. L. (1965) *J. Am. Oil Chem. Soc. 42*, 53.
Somerharju, P. J., & Wirtz, K. W. A. (1982) *Chem. Phys. Lipids 30*, 81-91.
Somerharju, P. J., van Paridon, P. A., & Wirtz, K. W. A. (1983) *Biochim. Biophys. Acta 731*, 186-195.
Somerharju, P. J., Virtanen, J. A., Eklund, K. K., Vaino, P., & Kinnunen, P. K. J. (1985) *Biochemistry 24*, 2773-2781.
Somerharju, P., Van Loon, D., & Wirtz, K. W. A. (1987) *Biochemistry 26*, 7193-7199.
Thompson, T. E. (1982) *J. Am. Oil Chem. Soc. 59*, 309A.
Trevelyan, W. G. (1966) *J. Lipid Res. 7*, 445-447.
Van Paridon, P. A., Visser, A. J. W. G., & Wirtz, K. W. A. (1987a) *Biochim. Biophys. Acta 898*, 172-180.
Van Paridon, P. A., Gadella, T. W. J., Somerharju, P. J., & Wirtz, K. W. A. (1987b) *Biochim. Biophys. Acta 903*, 68-77.
Wirtz, K. W. A. (1982) in *Molecular Biology of Lipid-Protein Interactions* (Griffith, O. H., & Jost, P. C., Eds.) Vol. 1, pp 151-231, Wiley-Interscience, New York.
Zborowski, J. (1979) *FEBS Lett. 107*, 30-32.
Zilversmit, D. B. (1984) *J. Lipid Res. 25*, 1563-1569.

Spectroscopic and Functional Characterization of an Environmentally Sensitive Fluorescent Actin Conjugate

Gerard Marriott,*,‡ Kasper Zechel,§ and Thomas M. Jovin‡
Abteilungen Molekulare Biologie und Biochemie, Max-Planck-Institut für Biophysikalische Chemie, Postfach 2841, D-3400 Göttingen, FRG

Received January 6, 1988; Revised Manuscript Received March 22, 1988

ABSTRACT: Rabbit skeletal muscle F-actin has been selectively labeled at a cysteine residue with the environmentally sensitive fluorophore 6-acryloyl-2-(dimethylamino)naphthalene. The fluorescent actin conjugate behaves similarly to native actin with respect to the polymerization kinetics, critical monomer concentration, and ability to form F-actin paracrystals. Upon polymerization to F-actin, the absorption of the actin conjugate is red-shifted, whereas the fluorescence emission is blue-shifted 740 wavenumbers and is accompanied by a decrease in the fluorescence bandwidth of 470 wavenumbers. These large shifts in the spectral properties of 6-propionyl-2-(dimethylamino)naphthalene (Prodan) in actin provide a simple method for obtaining a spectral discrimination between the G- and F-actin populations during the polymerization reaction. Steady-state fluorescence techniques were used to study the environment of the fluorophore in the monomeric and polymeric forms of actin. Fluorescence emission spectral analysis and quenching and polarization studies of G-actin–Prodan indicated that the fluorophore lies immobile on the protein surface but with one of its faces in full contact with the solvent. In F-actin, the fluorophore has a limited exposure to the solvent and is located in a dielectric environment similar to those seen for Prodan in polar, aprotic solvents or buried within a protein matrix [Macgregor, R. B., Jr., & Weber, G. (1986) *Nature (London) 318*, 70-73]. Additionally, our results demonstrate that the Prodan molecule conjugated to F-actin is completely immobile during its fluorescence lifetime, exhibits an increase in the resonance energy transfer (RET) from tryptophan residues compared to that observed in G-actin, and shows evidence of homologous RET within the polymer.

Numerous fluorescence spectroscopic techniques have been used to study structure–function relationships of actin and actin binding proteins (Cooper & Pollard, 1982; Frieden, 1985). Conformational transitions in the actin monomer during polymerization or ligand binding are often accompanied by a change in some fluorescence property of an intrinsic or extrinsic fluorophore. Virtually all fluorescence properties can be affected: the fluorescence quantum yield; the polarization of the fluorescence; the decay rate and/or rotational rate of the

* Author to whom correspondence should be addressed. Fellow of the Alexander von Humboldt Society.
‡ Abteilung Molekulare Biologie.
§ Abteilung Biochemie.

0006-2960/88/0427-6214$01.50/0

fluorophore (Wahl et al., 1975); the efficiency of resonance energy transfer between pairs of chromophores (Taylor et al., 1981); and the spectral energy of the emission. In studies of actin polymerization and ligation, the most popular of these techniques is based on a change in the quantum yield during the condensation reaction and is usually detected by monitoring the relative fluorescence intensity at the maximum wavelength of the fluorophore emission (Detmers et al., 1981; Wang & Taylor, 1980; Tait & Frieden, 1982). Although the fluorescence signal changes seen upon actin polymerization or ligand binding with the most commonly used fluorophores are easily and rapidly measured, they are rarely greater than a factor of 2 or 3 in relative magnitude, unless there are accompanying changes in the ground state of the fluorophore, e.g., the actin–pyrenylmaleimide conjugate (Kouyama & Mihashi, 1981). In protein systems where transitions may occur between two, three, or even more states, an analysis of the individual equilibria may be better served by using a fluorescent probe that exhibits changes not only in its emission intensity during a transition but also in spectral energy and bandwidth. We have initiated a study of fluorophores that display large spectral shifts to investigate protein complexation reactions so as to discriminate between different forms of the protein in an equilibrium. In particular, we have employed the fluorophore 6-propionyl-2-(dimethylamino)naphthalene (Prodan),[1] designed and synthesized by G. Weber (Weber & Farris, 1979). Prodan exhibits very large spectral shifts in both the absorption and emission that are dependent primarily on the dielectric environment of the fluorophore (Weber & Farris, 1979; Macgregor & Weber, 1981, 1986; Marriott, 1987). The present report demonstrates the use of this spectral shift probe in a study of actin polymerization using steady-state fluorescence techniques. Conclusions regarding the molecular environment of the probe are based on a detailed description of the steady-state fluorescence properties of the fluorophore in the two polymerization states of actin.

Materials and Methods

G-Actin was prepared from rabbit muscle as described in Spudich and Watt (1971). Actin was specifically labeled at a cysteine residue using Acrylodan (Molecular Probes, Eugene, OR), a thiol reactive adduct of Prodan (Prendergast et al., 1983). Prior to labeling of actin with Acrylodan, mercaptoethanol was removed from the protein storage buffer by dialysis against dialysis buffer (DB): 2 mM Tris-HCl, 0.2 mM ATP, and 0.1 mM $CaCl_2$, pH 7.9. Polymerization was initiated by the addition of $MgCl_2$ to a final concentration of 2 mM at 4 °C. After 2 h at 4 °C a 2 molar excess of Acrylodan in DMF was added in 10 aliquots over 10 min (the final volume of DMF was less than 0.2%). The reaction was left for 3 h at 4 °C, followed by dialysis for 60 h at 4 °C against DB containing 2 mM 2-mercaptoethanol (G buffer). The labeling ratio [dye]/[protein] was determined by using the extinction coefficient for actin at 290 nm of 2.6×10^4 $M^{-1}\cdot cm^{-1}$ (Gordon et al., 1976) and for Prodan at 375 nm of 1.85×10^4 $M^{-1}\cdot cm^{-1}$ (Weber & Farris, 1979). The protein concentration for the fluorescent conjugate was calculated after correction for the absorbance of Prodan at 290 nm; at this wavelength, the extinction coefficient is also 1.85×10^4 $M^{-1}\cdot cm^{-1}$. For the quenching studies of Prodan in actin, aliquots of a 2 M potassium iodide solution containing 1 mM sodium thiosulfite were added to the fluorescent actin preparations. The emission spectra were recorded immediately after the addition of iodide in order to minimize the effect of salt-induced polymerization. The integrated fluorescence intensities were corrected for dilution effects.

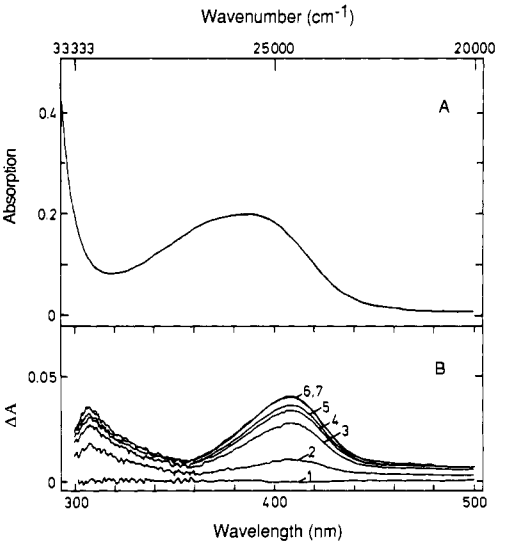

FIGURE 1: (A) Absorption spectrum of G-actin–Prodan (15 μM) in G buffer at 25 °C. (B) Time dependence of the absorption difference spectra of 20 μM G-actin–Prodan after the initiation of polymerization with 2 mM magnesium chloride. Each spectrum (1–7) was acquired over a 60-s period from the following times after initiation of polymerization: (1) 0 s; (2) 30 s; (3) 150 s; (4) 270 s; (5) 390 s; (6) 1050 s; and (7) 1830 s.

Viscosity measurements were made with an Ostwald-type viscometer described by Zechel (1981). Absorption spectra were recorded on a Kontron Uvicon 820 spectrophotometer. Fluorescence emission spectra were recorded on an SLM (Urbana, IL) Model 8000 spectrofluorometer with excitation at 380 nm (4-nm bandwidth) and emission collected between 400 and 650 nm (4-nm bandwidth). The emission data were corrected for the spectral response of the detection system. The spectra were analyzed in terms of the center of spectral mass in energy, defined by eq 1 (Torgerson et al., 1979) where ν_g

$$\nu_g = \sum \nu_i I_i / \sum I_i \quad (1)$$

is the average energy of the emission spectrum in reciprocal centimeters (cm^{-1}) and I_i is the fluorescence intensity at wavenumber ν_i. Steady-state fluorescence excitation polarization spectra were recorded on the same instrument in a 90° configuration with correction for the polarization response of the detection system. The spectra were measured with a 2-nm band-pass for excitation and an 8-nm band-pass for emission which was fixed at 495 nm. The Wood's anomalies inherent in the SLM excitation monochromator were removed by the introduction of a quartz depolarizer (Halle, Berlin) after the exit slit of the excitation monochromator.

Results and Discussion

Ground-State Properties of Prodan in G- and F-Actin. The absorption spectrum of G-actin–Prodan in G buffer at 25 °C is shown in Figure 1A. The labeling ratio [dye]/[protein] was 0.67. The absorption spectrum displays a broad maximum centered at approximately 375 nm (ν_g = 26 700 cm^{-1}) which is similar to that found for Prodan in aprotic, polar solvents such as propylene glycol at this temperature, for which ν_g is approximately 27 000 cm^{-1} (Marriott, 1987). The spectral bandwidth of Prodan in G-actin (3600 cm^{-1}) is somewhat

[1] Abbreviations: Acrylodan, 6-acryloyl-2-(dimethylamino)-naphthalene; ATP, adenosine 5′-triphosphate; DMF, dimethylformamide; DNase I, deoxyribonuclease I; FWHM, full width at half-maximum; Prodan, 6-propionyl-2-(dimethylamino)naphthalene; RET, resonance energy transfer; Tris, tris(hydroxymethyl)aminomethane.

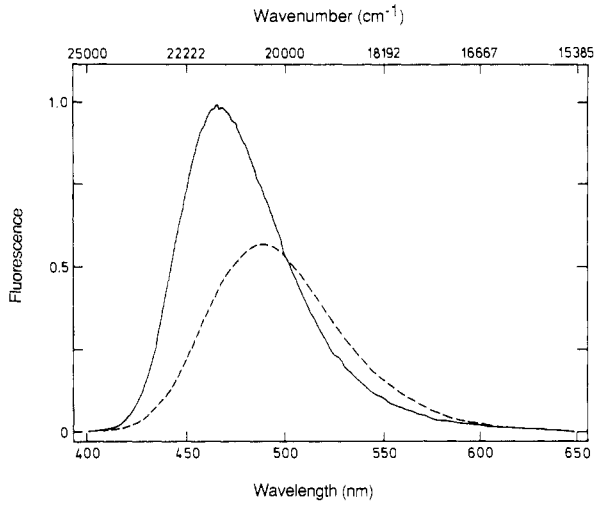

FIGURE 2: Corrected fluorescence emission spectra of 7.5 μM G-actin–Prodan in G buffer (---) and F-actin–Prodan (—) at 25 °C. The polymerization was induced by the addition to G-actin–Prodan of magnesium chloride to 2 mM.

larger than that seen in the pure, polar fluid solvents at 25 °C, such as ethanol, for which the FWHM is 2525 cm^{-1} (Weber & Farris, 1979). The larger absorption bandwidth of Prodan in the protein indicates a more heterogeneous ground-state molecular environment than in the pure, polar fluid solvents.

The kinetics of the polymerization process may be studied by using the time-dependent change in the absorbance difference spectrum illustrated in Figure 1B. The polymerization of G-actin–Prodan in G buffer was initiated by the addition of $MgCl_2$ to a final concentration of 2 mM (F buffer). The absorption spectrum of Prodan in F-actin is red-shifted compared to the monomer (Figure 1B), reflecting an energetically more favorable ground-state interaction with the protein. This red-shift results in a 1.4-fold increase in the molar extinction coefficient at 410 nm for Prodan in the polymer compared to G-actin. It is interesting to note that the relative signal change in the absorption of Prodan at 410 nm during the polymerization reaction is comparable or better than observed in the emission of some other fluorescent actin conjugates (Tait & Frieden, 1982; Wang & Taylor, 1980).

Fluorescence Emission Changes during the Polymerization of G-Actin–Prodan. The corrected fluorescence emission spectrum of G-actin–Prodan (Figure 2) in G buffer exhibits a maximum emission wavelength at 492 nm (ν_g = 20310 cm^{-1}), and after the completion of the polymerization process in F buffer (Figure 2), the maximum is shifted to 465 nm (ν_g = 21050 cm^{-1}). This demonstrates the large spectral shifts possible between protein conformations using this environmentally sensitive probe and provides an opportunity for accurately following the polymerization reaction. The spectral shift is also accompanied by a narrowing of the FWHM from 3600 to 3130 cm^{-1} and a 40% increase in the integrated relative fluorescence intensity for the polymer. The fluorescence bandwidths for Prodan in both actin species are very large compared to those observed in polar solvents such as DMF and ethanol, for which the FWHM values are 2723 and 2525 cm^{-1}, respectively (Weber & Farris, 1979). This comparison of the spectral bandwidths of Prodan in pure solvents and in the protein for the ground and excited states reveals that the molecular environments of the fluorophore in G- and F-actin are very heterogeneous and probably reflect the complex nature of the probe–protein–solvent interactions. In all our preparations of actin–Prodan, the average fluorescence energy for both G-actin and F-actin was reproducible to within 25

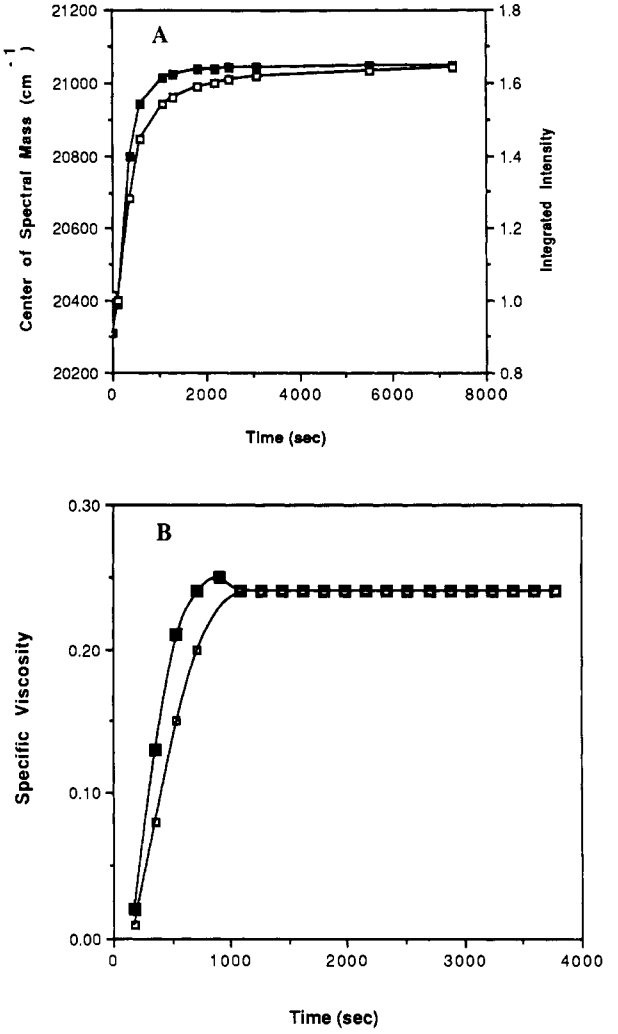

FIGURE 3: Time dependence of G-actin–Prodan polymerization. (A) Observation of fluorescence: average energy of the fluorescence emission (■); integrated relative fluorescence intensity (□). Each spectrum required a 150-s acquisition time. (B) Polymerization kinetics from the specific viscosity of native (□) and Prodan-labeled (■) G-actin. The protein concentration of both G-actin species was 5 μM. Each determination required 150 s of acquisition time.

wavenumbers of the values reported above. The constancy of this parameter for the different preparations suggests that there is a unique labeling site for the coupling conditions employed. It is known that the thiol group of cysteine-374 in actin reacts very fast with a variety of thiol reactive molecules (Martonosi, 1968) and it is this residue that Acrylodan presumably labels.

The time dependence of G-actin–Prodan polymerization seen through the fluorescence energy shift and the integrated fluorescence emission of Prodan are illustrated in Figure 3A. The small difference in the integrated relative fluorescence intensity between the two states allows us to ignore the intensity-dependent factor when calculating the concentration of the two actin species from the center of spectral mass. In those cases where a transition between two protein states results in a large change in the quantum yield in addition to a spectral shift, the deconvolution of the two fluorescence emission spectra must be performed as described in Torgerson et al. (1979). The large change in the center of spectral mass between the actin states allows an accurate determination of the concentrations of the two actin species in the solution at any time during the polymerization process. At present, however, our first full emission spectrum can be collected from time zero to 150 s after the initiation of polymerization. At times greater than 150 s, we have been able to fit the shape

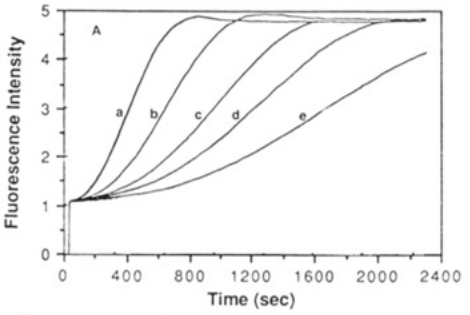

FIGURE 4: Concentration dependence of G-actin–Prodan polymerization kinetics at 25 °C. Actin–Prodan polymerization was observed by measuring a fluorescence signal biased for F-actin–Prodan. The excitation wavelength was 410 nm (4-nm bandwidth), and the emission was collected through a monochromator at 450 nm (8-nm bandwidth). The first data point was collected approximately 15 s after initiation of polymerization. The intensity-normalized curves correspond to G-actin–Prodan concentrations (micromolar) of (a) 6, (b) 4, (c) 3, (d) 2.5, and (e) 2.

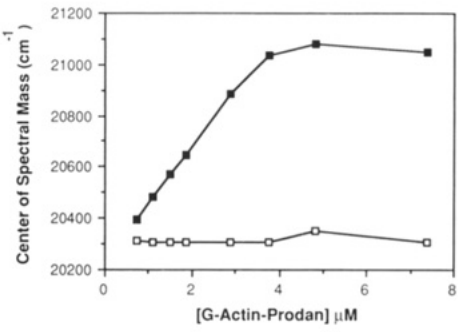

FIGURE 5: Determination of the critical monomer concentration for G-actin–Prodan. The average energy of the fluorescence emission was recorded against varying concentrations of G-actin–Prodan in G buffer (□) and F buffer 90 min after the addition of $MgCl_2$ (■). The critical monomer concentration was obtained from the intersection of the two curves.

of the corrected emission spectra using a computer program that adds varying amounts of reference G-actin–Prodan and F-actin–Prodan spectra. The residuals from such a two-component shape fit are very small and suggest that at times greater than 150 s after the induction of polymerization, there are no actin species other than G- and F-actin present at concentrations greater than a few percent of the initial G-actin concentration. We note that the use of a multichannel detection system would allow a similar analysis of the protein composition of the actin pool at earlier times in the polymerization process. However, even with conventional fluorescence instrumentation, the spectral shifts between the ground and excited states of Prodan in actin can be exploited to obtain a high degree of spectral discrimination between the two actin species during the initial stages of the polymerization through judicious choices of the excitation and emission wavelengths. For example, with excitation and emission at 410 and 440 nm, respectively, the fluorescence signal for equimolar concentrations of the two actin–Prodan species is slightly more than 5 to 1 in favor of the polymer. Additionally, if the ratio of the emission at 440 and 550 nm is measured during polymerization, the discrimination factor increases to nearly 8-fold. The concentration dependence of G-actin–Prodan for the polymerization process measured with an F-actin–Prodan-biased signal and manual mixing is shown in Figure 4. We are currently performing a detailed study of actin–Prodan polymerization kinetics with this F-actin–Prodan-biased signal using approaches similar to those reviewed by Frieden (1985).

Functional Integrity of G-Actin–Prodan and F-Actin–Prodan. We have established the functional integrity of the fluorescent actin conjugate by measuring the high shear viscosity during the polymerization reaction of native and fluorescent actin. The progress of the polymerization reaction observed by changes in the specific viscosity (Figure 3B) indicates that the Prodan moiety does not appreciably impair the polymerization properties of the protein; neither the rate of polymerization nor the reduced viscosity obtained after polymerization (η/c = 11.5 dL g^{-1}) differs significantly between the native and fluorescent actin. G-Actin–Prodan and native G-actin both exhibited similar Stokes radii as determined by size-exclusion chromatography. We have also established the similarity in properties between the native and labeled actin through a determination of the critical polymerization concentration (Figure 5). The critical monomer concentration for G-actin–Prodan of 0.2 μM is in good agreement with the values determined for native actin (Gordon et al., 1977) and for other fluorescent actin conjugates [e.g., see Wegner (1982) and Kouyama and Mihashi (1981)]. A further example of the functional integrity of the actin–Prodan conjugate was provided by its ability to form paracrystals in 25 mM $MgCl_2$ (Aebi et al., 1980), a fluorescence micrograph of which is shown in Figure 6.

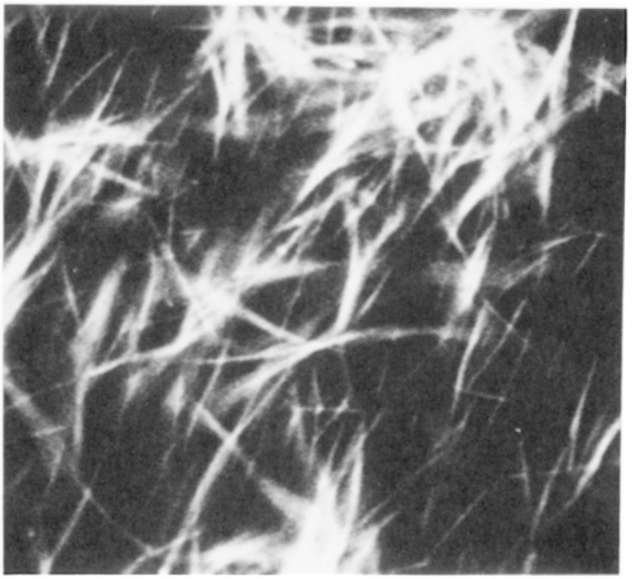

FIGURE 6: Fluorescence micrograph of F-actin–Prodan paracrystals in 25 mM $MgCl_2$ at 25 °C. Excitation wavelength was 365 nm, and the emission was collected through a 450-nm interference filter.

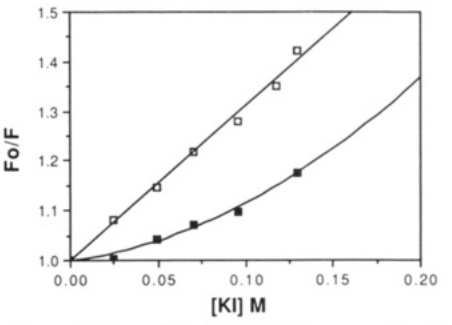

FIGURE 7: Stern–Volmer plot of the iodide quenching behavior of Prodan in G-actin (□) and F-actin (■). G-Actin–Prodan and F-actin–Prodan were both present at 4 μM at 25 °C.

Molecular Environment of Prodan in G-Actin. Information on the molecular environment of the probe in G-actin may be deduced from fluorescence quenching studies (Tao & Cho, 1979), fluorescence polarization measurements, and an analysis of the fluorescence emission spectrum. An iodide quenching

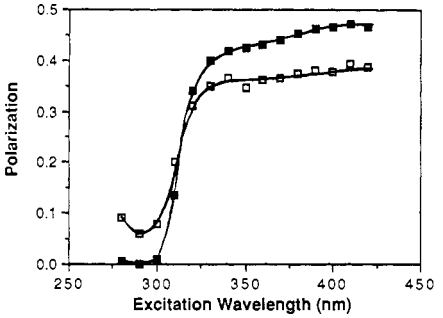

FIGURE 8: Fluorescence excitation polarization spectra of Prodan in G-actin (□) and F-actin (■). Polarization values were recorded every 10 nm from 280 to 420 nm as described in the text. The error in each measurement was ±0.001 polarization unit. Conditions were as in Figure 7.

study of G-actin–Prodan (Figure 7) suggests that the probe is fully exposed to the solvent, since iodide ions quench with a bimolecular rate constant close to diffusion-controlled (7.5×10^8 $M^{-1}\cdot s^{-1}$) if we assume the fluorescence lifetime of Prodan in the protein is 4 ns (Marriott, 1987). The average energy of the fluorescence emission for G-actin–Prodan at iodide concentrations up to 0.13 M is blue-shifted by only 80 cm^{-1}. This shift is probably due to a small amount of salt-induced polymerization and indicates that the blue-edge and red-edge spectral populations of Prodan in G-actin are equally quenched, as expected if all the Prodan molecules are equally exposed to the solvent. Furthermore, the uniform rate of iodide quenching rates for Prodan conjugated to G-actin suggests that the large environmental heterogeneity of the Prodan previously discussed does not include a mixed contribution from chromophores that are partially and fully buried but must originate from the interactions of a unique species with the protein surface and the solvent milieu.

Prodan demonstrates a unique absorption transition moment (S_0–S_1) from approximately 320 to 450 nm (Weber & Farris, 1979). The excitation polarization spectrum of Prodan in G-actin in G buffer at 25 °C is shown in Figure 8. The steady-state polarization value with red-edge excitation for G-actin–Prodan is high (p of 0.38), indicating that the fluorophore has little rotational freedom within the protein. In fact, the residual depolarization can be accounted for through the global tumbling of the protein (Weber, 1952). This result, together with the findings of the iodide quenching study, suggests that the probe lies immobile on the protein surface and probably one of its faces is fully accessible to the solvent.

A comparison of the fluorescence excitation polarization spectra for Prodan in G-actin (Figure 8) and in a viscous solvent such as glycerol (Weber & Farris, 1979) reveals a significant reduction in the polarization value for the G-actin conjugate in the spectral region 280–300 nm; this could arise from intramolecular RET between the tryptophan residues of G-actin and the Prodan moiety. RET is expected in this protein system since actin has four tryptophan residues per monomer and there is a large spectral overlap between the emission of tryptophan with the absorption of Prodan (Marriott, 1987).

Molecular Environment of Prodan in F-Actin. The fluorescence emission characteristics of F-actin–Prodan provide a description of the molecular environment of the probe in the polymer. The origin of the 740 cm^{-1} spectral energy shift observed after G-actin–Prodan polymerization is related to a decrease in the polarizability of the molecular environment of the probe in F-actin. The dielectric environment of the probe in the polymer can be correlated with its center of spectral mass (Figure 2), and the value of 21 150 cm^{-1} is similar to that found for Prodan in polar, aprotic solvents such as DMF, for which ν_g is 21 700 cm^{-1} (Weber & Farris, 1979). Since DMF has a similar dipole moment (3.5 D) as a peptide bond (3.7 D), one interpretation of the disposition of the probe in the polymer is that it is buried within the protein. In this regard, our results support the findings from other workers on the surface accessibility of the thiol group of cysteine-374 in F-actin (Uyemura & Spudich, 1980; Taylor et al., 1981), although we believe that after the coupling reaction the hydrophobic fluorophore becomes buried within the protein or at an actin–actin interface. This hypothesis is supported by the observation that the average energy of the emission and the fluorescence bandwidth of Prodan in F-actin are similar to those seen for Prodan deeply buried in other protein environments such as the heme pocket of apomyoglobin, in which case ν_g is 21 755 cm^{-1} (Macgregor & Weber, 1986), the apolar binding site(s) of BSA, for which ν_g is 21 322 cm^{-1} with a FWHM of 3380 cm^{-1} (Weber & Farris, 1979), and covalently attached to a cysteine residue in HSA, for which ν_g is 21 025 cm^{-1} with a FWHM of 3756 cm^{-1} (Marriott, 1987). Further information about the molecular environment of the probe in the polymer can be derived from iodide quenching studies of F-actin–Prodan. The iodide quenching behavior of Prodan in the polymer (Figure 7) appears complex when analyzed in terms of a Stern–Volmer plot (Stern & Volmer, 1919), although it is clear that there is a marked reduction in the quenching efficiency compared to the monomer. This indication of the removal of the probe from contact with the solvent upon polymerization is consistent with the dielectric environment of the probe deduced from the emission spectra analysis. The complex nature of the iodide quenching curve for F-actin–Prodan may be due to static quenching, responsible for the upward curvature of the quenching curve, or to a population of the probe molecules that are inaccessible to the solvent (Lehrer, 1971). Alternatively, there may occur a partial depolymerization of F-actin–Prodan, since a reversible dissociation of the polymer is mediated by high potassium iodide concentrations (Szent Gyorgyi, 1951).

The excitation polarization spectrum of F-actin–Prodan (Figure 8) gives a polarization of 0.465 with red-edge excitation. This value, which approaches the limiting polarization for Prodan of 0.47 is a further indication of a reduction in the mobility of the probe in the polymer with respect to monomeric actin. Consequently, there must be a complete absence of rotational motion of the probe and the individual subunits in F-actin–Prodan during the fluorescence lifetime of Prodan. Figure 8 also shows a zero polarization value in the spectral region from 280 to 300 nm, partly due to an increased efficiency in the RET from the tryptophan residues to the Prodan moiety in the polymer compared to that observed in the monomeric conjugate. This increase in the RET efficiency may result from a number of factors, including changes in the relative orientation factor between one or more tryptophan residues and Prodan within each subunit, and an additional contribution from intermolecular RET. Finally, from Figure 8 the steady increase in the polarization value across the blue-edge of the S_0–S_1 transition for F-actin–Prodan suggests the presence of a homologous RET (Anderson & Weber, 1969) between Prodan molecules on neighboring actin molecules. An RET study between subunits in F-actin using donor–acceptor pairs of fluorescent actin conjugates has been reported by Taylor et al. (1981). In homo-energy transfer, however, there must be a spectral overlap between the blue-emitting donor Prodan molecules with the red-edge (of the absorption) Prodan acceptor molecules. In the case of F-ac-

tin-Prodan, an inspection of the spectral overlap between the absorption and emission spectra (Figures 1A and 2) would indicate that this integral is rather small. Consequently, the fact that energy transfer exists at all must be due to a very favorable alignment of the absorption and emission oscillators of Prodan molecules along the polymer; that is, a high degree of spatial order must exist between neighboring absorption and emission dipoles of Prodan in the filament. The absence of any rotational motion of Prodan in the polymer allows us to calculate an average angular displacement between the dipoles of a Prodan donor-acceptor pair involved in RET of approximately 13° (Jablonski, 1952). Whether the Prodan transfer pairs consist of adjacent actin molecules on a single filament and/or two protomers on adjacent actin filaments is not known from this study although Taylor et al. (1981) have reported the presence of RET only between filaments.

Conclusion

We have investigated the use of the spectral shift of a fluorescence probe in a study of the actin polymerization reaction. The ability to isolate the fluorescence spectra of the two actin species due to shifts in the absorption and emission could have a large potential in resolving the complex kinetic mechanism of actin polymerization. In particular, such a technique will be of great use in steady-state fluorescence emission microscopy. For example, the spectral shifts observed for actin-Prodan allow an 8-fold signal discrimination for equal concentrations of the monomer and polymer. Furthermore, in the case of two-state systems for which Prodan exhibits larger spectral shifts, these factors can be even greater. Although this large fluorescence signal discrimination would not appear to be an important requirement for studying the kinetics of actin polymerization in vitro, for which the equilibrium constant for the polymerization process is heavily biased toward the polymeric state, such a situation is unlikely to exist in vivo. For example, there are over 40 actin binding proteins described in the literature (Stossel et al., 1985) that are found in cells of various origin, some of which may be present at cellular concentrations comparable to that of actin. The dissociation constants of these actin binding proteins range from 10^{-9} to 10^{-6} M (Stossel et al., 1985). On the basis of these facts, the idea that G-actin is present as a distinct entity in cells appears unlikely; rather, one expects at any given time in a cell there will exist an appreciable amount of unpolymerized but complexed actin. In fluorescence microscopy studies of living cells employing microinjected fluorescent actin conjugates that are relatively insensitive to the state of polymerization, there will be a large fluorescence originating from these nonpolymerized fluorescent actin complexes. If so, the fluorescence signal originating from the polymeric actin will be relatively small, and the image of the actin filaments will appear diffuse. In the case of actin-Prodan, however, the signal contribution from nonpolymerized actin complexes in which the G-actin-Prodan fluorescence remains unperturbed, e.g., DNase I (Marriott, unpublished results), can be reduced up to 8-fold through the separate detection and ratioing of the 440- and 550-nm fluorescence signals. Another situation that highlights the advantages of using spectral shift probes in fluorescence microscopy is the case of a fluorescent biopolymer that may exist in two conformationally distinct forms, for example, as a result of ligand binding or protein complexation. In these situations, the isolation of the signal from one or both polymeric states using steady-state fluorescence microscope imaging techniques with dielectrically insensitive fluorophores will be almost impossible. However, if in the case of a Prodan-labeled polymer there is a shift in the absorption and/or fluorescence emission between the two forms as a result of ligation or complexation, then, depending on the magnitudes of the shifts, it should be possible to image the spatial distribution of one or both polymers.

Finally, the requirements for fluorescence imaging through steady-state polarization measurements using natural light excitation as proposed by Weber (1985) require an ordered alignment of the absorption dipoles of an immobile fluorophore in a polymer. We have shown that this condition may be satisfied for Prodan in F-actin filaments as evidenced by the existence of homo-energy transfer.

Acknowledgments

We thank Dr. Robert Clegg for helpful discussions and Dr. Michel Robert-Nicoud for help with fluorescence microscopy.

Registry No. Acrylodan, 86636-92-2; Prodan, 70504-01-7.

References

Aebi, U., Smith, P. R., Isenberg, G., & Pollard, T. D. (1980) *Nature (London) 288*, 296–298.
Anderson, S., & Weber, G. (1969) *Biochemistry 8*, 371–377.
Cooper, J. A., & Pollard, T. D. (1982) *Methods Enzymol. 85*, 182–210.
Detmers, P., Weber, A., Elzinga, M., & Stephens, R. E. (1981) *J. Biol. Chem. 256*, 99–105.
Frieden, C. (1985) *Annu. Rev. Biophys. Biophys. Chem. 14*, 189–210.
Gordon, D. J., Yang, Y.-Z., & Korn, E. D. (1976) *J. Biol. Chem. 251*, 7474–7479.
Gordon, D. J., Boyer, J. L., & Korn, E. D. (1977) *J. Biol. Chem. 252*, 8300–8309.
Jablonski, A. (1952) *Z. Phys. 106*, 526–532.
Kouyama, T., & Mihashi, K. (1981) *Eur. J. Biochem. 114*, 33–38.
Lehrer, S. S. (1971) *Biochemistry 10*, 3254–3263.
Macgregor, R. B., Jr., & Weber, G. (1981) *Ann. N.Y. Acad. Sci. 366*, 140–154.
Macgregor, R. B., Jr., & Weber, G. (1986) *Nature (London) 318*, 70–73.
Marriott, G. (1987) Ph.D. Thesis, University of Illinois.
Martonosi, A. (1968) *Arch. Biochem. Biophys. 723*, 29–40.
Prendergast, F. G., Meyer, M., Carlson, G. L., Iida, S., & Potter, J. D. (1983) *J. Biol. Chem. 258*, 7541–7544.
Spudich, J. A., & Watt, S. (1971) *J. Biol. Chem. 246*, 4866–4871.
Stern, O., & Volmer, M. (1919) *Z. Phys. 20*, 183–187.
Stossel, T. P., Chaponnier, C., Ezzel, R. M., Hartwig, P. A., Janmey, P. A., Kwiatkoswski, D. J., Lind, S. E., Smith, D. B., Southwick, F. S., Lin, H. L., & Zaner, K. S. (1985) *Annu. Rev. Cell Biol. 1*, 353–402.
Szent Gyorgyi, A. G. (1951) *Arch. Biochem. Biophys. 31*, 97–103.
Tait, J. F., & Frieden, C. (1982) *Arch. Biochem. Biophys. 216*, 133–138.
Tao, T., & Cho, J. (1979) *Biochemistry 18*, 2759–2765.
Taylor, D. L., Reidler, J., Spudich, J. A., & Stryer, L. (1981) *J. Cell Biol. 89*, 362–367.
Torgerson, P. M., Drickhammer, H. G., & Weber, G. (1979) *Biochemistry 18*, 3079–3082.
Uyemura, D., & Spudich, J. A. (1980) in *Biological Regulation and Development* (Goldberger, R., Ed.) Vol. 2, pp 317–338, Plenum, New York.
Wahl, Ph., Mihashi, K., & Auchet, J. C. (1975) *FEBS Lett. 60*, 164–167.

Wang, Y. L., & Taylor, D. L. (1980) *J. Histochem. Cytochem. 28*, 1198-1206.
Weber, G. (1952) *Biochem. J. 51*, 145-155.
Weber, G. (1985) in *Applications of Fluorescence in the Biomedical Sciences* (Taylor, D. L., Waggoner, A. S., Murphy, R. F., Lanni, F., & Birge, R. R., Eds.) pp 601-615, Alan R. Liss, New York.
Weber, G., & Farris, F. (1979) *Biochemistry 18*, 3075-3078.
Wegner, A. (1982) *J. Mol. Biol. 161*, 607-615.
Zechel, K. (1981) *Eur. J. Biochem. 119*, 209-213.

Study of the Effect of Poly(L-lysine) on Phosphatidic Acid and Phosphatidylcholine/Phosphatidic Acid Bilayers by Raman Spectroscopy†

Gaëtan Laroche, Danielle Carrier,‡ and Michel Pézolet*
Centre de Recherche en Sciences et en Ingénierie des Macromolécules, Département de Chimie, Université Laval, Cité Universitaire, Québec, Canada G1K 7P4

Received January 21, 1988; Revised Manuscript Received April 8, 1988

ABSTRACT: The effect of polylysine (PLL) on dimyristoylphosphatidic acid (DMPA), on dimyristoylphosphatidylcholine (DMPC), and on mixtures of these lipids was investigated by Raman spectroscopy. These results show that long polylysine ($M_r \approx 200\,000$) increases the stability of the acyl chain matrix of DMPA to form a more closely packed structure with a stoichiometry of one lysine residue per PA molecule. On the other hand, short PLL (M_r 4000) destabilizes the PA bilayer, and the complex formed undergoes a gel to liquid-crystalline transition at a lower temperature than of the pure lipid. For both cases, we have observed that bound polylysine adopts a β-sheet conformation as opposed to the α-helical structure previously found for dipalmitoylphosphatidylglycerol/long PLL complexes [Carrier, D., & Pézolet, M. (1984) *Biophys. J. 46*, 497-506]. The difference in the thermal behavior of complexes of DMPA with long and short polylysines is believed to be associated with the fact that in the complex the long polypeptide adopts the β-sheet conformation over the whole range of temperatures investigated while the short one undergoes a change of conformation from β-sheet of random coil upon heating. Therefore, the conformation of the lipid-bound polypeptides depends on the nature of the polar head group of the lipid, not only on its net charge, and it affects considerably the thermotropism of the lipid. On the other hand, both long and short polylysines show no affinity for phosphatidylcholine since the temperature profiles of DMPC and of DMPC/PLL complexes exhibit exactly the same behavior. When mixed with PA/PC mixtures, long PLL induces a partial lateral phase separation. One phase consists mainly of DMPC but contains some DMPA, and the second phase is richer in the PA component and is perturbed by PLL. On the contrary, short polylysine does not induce phase separation as both lipids of the mixture exhibit the same thermotropic behavior.

The miscibility of membrane lipids and the occurrence of lateral phase separation are of prime interest in the study of membrane structure and function. The organization of membrane lipids in domains has been detected in almost all bacteria and cells of complex organisms, with the exception of erythrocytes (Karnovsky et al., 1982). It has even been observed in the viral membrane of the influenza mixovirus (Bukrinskaya et al., 1987). This heterogeneity seems to have a functional significance. For example, one of the first requirements for the fusion between membranes is believed to be the presence of specific local domains (Portis et al., 1979; Scheule, 1987).

Lateral phase separation in a membrane can be induced by external agents like multivalent cations, among which calcium has been extensively studied (Onishi & Ito, 1974; Jacobson & Papahadjopoulos, 1975; Galla & Sackmann, 1975a,b; Van Dijck et al., 1978; Hui et al., 1983; Silvius & Gagné, 1984a,b; Kouaouci et al., 1985). Polycationic species can also be very effective, and one of the most studied is poly(L-lysine) (PLL),[1] a polypeptide often taken as a model of extrinsic protein. PLL-induced phase separation was first observed in dipalmitoylphosphatidic acid bilayers, by electron spin resonance and fluorescence spectroscopy (Galla & Sackmann, 1975a,b; Hartmann & Galla, 1978; Hartmann et al., 1977). The formation of domains of bound phosphatidic acid within the pure phospholipid, or in mixtures with dioleoylphosphatidylcholine, has also been proved by electron microscopy (Hartmann et al., 1977). Later, PLL was shown to induce a very peculiar behavior in dipalmitoylphosphatidylglycerol bilayers, where three types of domains were observed for a lipid to lysyl residue ratio greater than 1 (Carrier & Pézolet, 1985). A fundamental finding of the same study is that the degree of polymerization of the peptide is very important when dealing with the structure and thermotropism of phosphatidylglycerol/PLL complexes. In fact, long polylysine (M_r >150 000) causes a shift of the gel to liquid-crystalline tran-

† This research was supported in part by the National Science and Engineering Research Council of Canada (M.P.) and the Fonds FCAR, Province of Québec (M.P.). G.L. was the recipient of a scholarship from the National Science and Engineering Research Council of Canada.
‡ Present address: Division of Chemistry, National Research Council, Ottawa K1A 0R6, Canada.

[1] Abbreviations: DMPA, dimyristoylphosphatidic acid; DMPC, dimyristoylphosphatidylcholine; DMPC-d_{54}, DMPC with perdeuteriated acyl chains; DMPG, dimyristoylphosphatidylglycerol; DPPG, dipalmitoylphosphatidylglycerol; EDTA, ethylenediaminetetraacetic acid; PLL, poly(L-lysine); R_i, phospholipid to lysine residue incubation molar ratio.

0006-2960/88/0427-6220$01.50/0